Structure *14*, 737–748, April 2006 DOI 10.1016/j.str.2006.01.009

The Structure of a Ketoreductase Determines the Organization of the β-Carbon Processing Enzymes of Modular Polyketide Synthases

Adrian T. Keatinge-Clay[1,*] and Robert M. Stroud[1]
[1] Department of Biochemistry and Biophysics
University of California, San Francisco
600 16th Street
San Francisco, California 94107

Summary

The structure of the ketoreductase (KR) from the first module of the erythromycin synthase with NADPH bound was solved to 1.79 Å resolution. The 51 kDa domain has two subdomains, each similar to a short-chain dehydrogenase/reductase (SDR) monomer. One subdomain has a truncated Rossmann fold and serves a purely structural role stabilizing the other subdomain, which catalyzes the reduction of the β-carbonyl of a polyketide and possibly the epimerization of an α-substituent. The structure enabled us to define the domain boundaries of KR, the dehydratase (DH), and the enoylreductase (ER). It also constrains the three-dimensional organization of these domains within a module, revealing that KR does not make dimeric contacts across the 2-fold axis of the module. The quaternary structure elucidates how substrates are shuttled between the active sites of polyketide synthases (PKSs), as well as related fatty acid synthases (FASs), and suggests how domains can be swapped to make hybrid synthases that produce novel polyketides.

Introduction

Modular PKSs are multienzyme factories, expressed principally in actinomycetes, that synthesize a vast array of complex molecules, including many important pharmaceuticals (O'Hagan, 1991; Staunton and Wilkinson, 1997; Staunton and Weissman, 2001). The soil bacteria *Streptomyces erythraea* uses a modular PKS to fuse simple carbon building blocks into the antibiotic erythromycin. In assembly line fashion, each of the six modules of the erythromycin synthase condenses a 3-carbon methylmalonyl extender unit onto a polyketide chain initiated by a propionyl primer unit, yielding the 21-carbon precursor of erythromycin, 6-deoxyerythronolide B (6-dEB) (Figure 1) (Donadio and Katz, 1992). Within a module, an extender unit is selected by an acyltransferase (AT), shuttled by an acyl carrier protein (ACP) via an ~18 Å long phosphopantetheinyl arm, and condensed to the growing polyketide chain by a ketosynthase (KS).

Three β-carbon processing enzymes can act on the β-keto group formed after each condensation: KR uses NADPH to stereospecifically reduce it to a hydroxyl group, DH removes the hydroxyl group to create a double bond, and ER uses NADPH to reduce the double bond. In this way, a methylene functionality is produced by a complete module, which contains each of these enzyme activities. To create a more functionalized ketide unit, enzymes acting on the β-carbon are either inactive or absent from the module that controls its addition to the growing polyketide chain.

While some successes in engineering modular PKSs to produce novel polyketides have been reported, the majority of engineered synthases are nonfunctional. A major obstacle is the lack of structural information. Clear boundaries between domains have not been described, and little is known about the interfaces between domains. For example, in order to introduce new extender units into a polyketide chain, chimeric modules have been constructed in which the AT has been replaced with an AT of different substrate specificity. However, the incorporated AT usually shows diminished specificity and catalytic efficiency, most likely due to structural perturbation of that domain (Ruan et al., 1997).

The structure of an ER fragment has been reported (Gogos et al., 2003). However, all other structural information on modular PKSs comes from outside the boundaries of the module—from the structures of docking domains that connect the module-containing proteins (Broadhurst et al., 2003) and of thioesterases (TEs) located after the final module (Tsai et al., 2001, 2002). The most accepted model for the higher-order structure of PKSs is a dimeric, head-to-head, tail-to-tail organization (Staunton et al., 1996). It is supported by the dimeric structures of TE and the docking domains, as well as by limited proteolysis experiments of proteins from the erythromycin synthase (also called the 6-dEB synthase or DEBS), which revealed that fragments containing neighboring KS and AT are dimeric (Staunton and Weissman, 2001). In the head-to-head, tail-to-tail model, it is proposed that KS and AT form the center of the module, while some or all of DH, ER, KR, and ACP do not make contact across the 2-fold axis of the module. The domains always occur in the same order: KS, AT, DH, a large interdomain linker (Bedford et al., 1996), ER, KR, and ACP. Animalian FASs, which are believed to be structurally homologous to complete PKS modules, also contain these domains. Reconstructions of the human FAS from electron micrographs reveal a head-to-head, tail-to-tail dimer (Asturias et al., 2005).

Ideally, to determine the arrangement of domains within a module, a complete module would be crystallized and its structure solved. However, the connections between domains of a complete module (~440 kDa) might be flexible and impede crystallization. We decided to dissect a module into stable domains and crystallize them, focusing on a modular fragment that would be informative about domain boundaries and their organization within a module. The large interdomain linker and the "KR" region always appear together and are present in greater than 95% of the modules. In a full module, they border DH, ER, and ACP. Hybrid synthases containing a KR replacement have only been successful when the large interdomain linker was included, yet its function was unclear (Bedford et al., 1996; McDaniel et al., 1997). In limited proteolysis experiments of DEBS1, a stable fragment that contains the large interdomain linker and the "KR" region from the first module was

*Correspondence: adriankc@msg.ucsf.edu

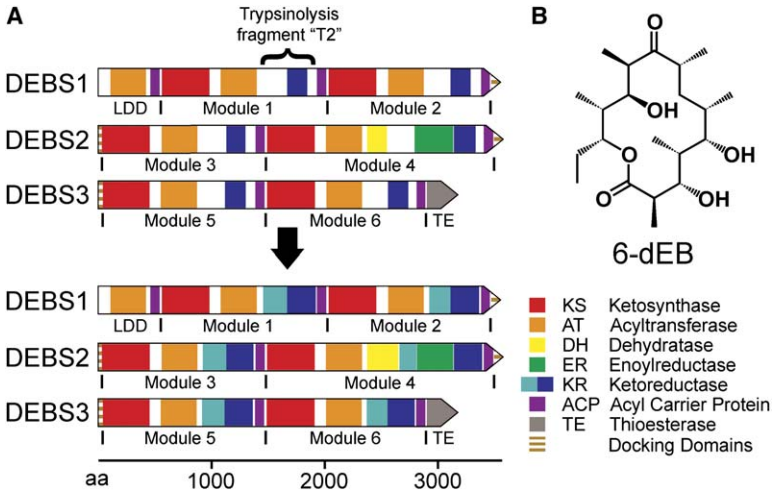

Figure 1. The Erythromycin Synthase Domain Structure

(A) Domains with predicted or known structure are colored, while regions that have no hypothesized structure are white. The structure of the T2 trypsinolysis fragment presented here allowed for the adjustment of domain boundaries, as indicated by the arrow. LDD, loading didomain.

(B) The synthase produces 6-deoxyerythronolide B (6-dEB), a precursor of erythromycin.

identified and labeled "T2" (Figure 1) (Aparicio et al., 1994). Recently, several fragments from the erythromycin and tylactone synthases with boundaries based on T2 were isolated and demonstrated to retain KR activity (Siskos et al., 2005).

We determined the structure of the T2 fragment. It is monomeric but composed of two subdomains, each resembling an SDR monomer (Oppermann et al., 2003). The large interdomain linker forms a structural subdomain, while the "KR" region and 70 residues C-terminal to it form a catalytic subdomain. The locations of the N- and C-termini, as well as a loop into which ER is inserted when present, enabled us to position the β-carbon processing enzymes and ACP relative to each other. The isolated KR domain is an active reductase and may double as an epimerase. Two residues hypothesized to be important in controlling the stereochemistry of ketoreduction are not essential for catalysis. The structural and catalytic details presented are applicable to the highly related animalian FAS.

Results

Initial Characterization and Crystallography

The region encoding T2 was cloned from a plasmid harboring a synthetic version of *eryAI* (the DEBS1 gene) with codons optimized for *Escherichia coli* (Kodumal et al., 2004). It was expressed in *E. coli* BL21(DE3), purified, and shown to be monomeric by both analytical ultracentrifugation and gel filtration (Figure S1; see the Supplemental Data available with this article online). Crystals of the apoprotein grew but did not diffract beyond 6 Å. After rescreening in the presence of 5 mM NADPH, a condition was identified in which two crystal forms were obtained, both diffracting beyond 2 Å. The structure was solved by using selenomethionine-labeled protein by single-wavelength anomalous dispersion (Table 1). Crystals could be grown or soaked with diketide substrate and product analogs, but no corresponding density was observed.

Overall Structure

The large interdomain linker and the "KR" region both adopt folds similar to those observed in members of the SDR family of enzymes (Jornvall et al., 1995; Oppermann et al., 2003) and associate to form one stable domain (Figure 2). However, only the "KR" region binds NADPH and has the conserved catalytic residues observed in other SDR enzymes. The structure reveals that the ~100 residues C-terminal to the catalytic tyrosine are part of the catalytic portion. This extends the C-terminal boundary of KR ~70 residues from its former placement. The "KR" region and this C-terminal region will be referred to as the catalytic subdomain of KR. The subdomain formed by the large interdomain linker appears to have a purely structural role and will be referred to as the structural subdomain of KR. Thus, the KR domain is comprised of a structural subdomain and a catalytic subdomain.

When the structure was compared to other enzymes in the Protein Data Bank, it was found to be most structurally homologous to the dehydrogenase portion of rat peroxisomal multifunctional enzyme 2 (MFE-2) (PDB code: 1GZ6), which helps oxidize fatty acids in a β-oxidation pathway (Holm and Sander, 1996; Haapalainen et al., 2003). This enzyme is dimeric, and each monomer possesses a C-terminal β-strand that spans both monomers. These two β-strands apparently strengthen the dimer by bridging the β-sheets of the monomers, in a manner similar to how β1 and β8 bridge the structural and catalytic subdomains of KR (Figure 2B).

The structural subdomain of KR begins with the bridging β-strand β1, which contains a (H/L/M/F/Y)XXXW sequence motif. This sequence serves as an important landmark by which to identify the start of KR since there is very little sequence conservation in the structural subdomain. The few conserved residues in the structural half clearly serve a structural role (primarily on α3, α4, β1, β7, and β8, such as T1572, G1594, E1602, and R1649). Compared to the catalytic subdomain, the structural subdomain is missing αC and βC. The second bridging β-strand, β8, exits the structural subdomain toward a loop that begins the Rossmann fold of the catalytic subdomain. The fold finishes with a series of short helices ending 12 residues from ACP.

A long groove runs from the top of NADPH to αH (Figure 2C). The adenine ring of NADPH and its ribose have similar temperature factors to that of the protein,

Table 1. Crystallization Data and Refinement Statistics

	Seleno-Protein	Native	Native
Data Collection			
Space group	P1	P1	P1
Cell dimensions			
a, b, c (Å)	44.0, 47.3, 63.3	43.2, 46.3, 61.5	42.0, 42.9, 61.0
α, β, γ (°)	94.6, 89.5, 97.9	94.7, 90.2, 98.9	90.0, 103.8, 100.7
Resolution (Å)	50–2.30	50–1.81	50–1.79
R_{merge}	0.069 (0.254)	0.058 (0.302)	0.061 (0.320)
$I/\sigma(I)$	10.8 (4.4)	8.1 (2.0)	8.1 (2.0)
Completeness (%)	96.4 (91.4)	93.7 (80.9)	94.2 (84.7)
Redundancy	1.5 (1.3)	1.8 (1.6)	1.8 (1.6)
Refinement			
Resolution (Å)	50–2.30	50–1.81	50–1.79
Number of reflections	24,037	40,140	36,130
R_{work}/R_{free}		0.235/0.263	0.227/0.257
Number of atoms			
Protein		3,458	3,382
NADPH		48	48
Water		180	236
B factors			
Protein		34	34
NADPH		50	56
Water		38	44
Rms deviations			
Bond lengths (Å)		0.007	0.007
Bond angles (°)		1.2	1.2

although the nicotinamide half is invisible in the electron density maps. The adenine ring stacks against R1698 and hydrogen bonds to D1726 and V1727. The adenine ribose phosphate hydrogen bonds to S1699 and forms a salt bridge with R1698. As in many SDR enzyme structures, part of the substrate binding site is disordered (Price et al., 2004). In one crystal form, αFG is invisible, and, in the other, its temperature factors are elevated.

The catalytic tyrosine, Y1813, and serine, S1800, are positioned similar to other SDR enzymes (Figure 3) (Oppermann et al., 2003). However, P1815 breaks αF so that Y1813 is not in the helix as in other SDR enzymes. Also, compared to other SDR structures, the positions of the conserved lysine, K1776, and asparagine, N1817, are swapped. Even so, the K1776 amine forms the same interaction observed in other SDR enzymes, hydrogen bonding with the backbone carbonyl 2 residues N-terminal of the catalytic serine. The N1817 side chain hydrogen bonds to the Y1813 backbone carbonyl.

Control in Catalysis

Recent enzymology of isolated KRs demonstrated that incubation of the first KR of the erythromycin synthase with an unreduced diketide mixture (the α-substituent slowly epimerizes in solution) resulted in the exclusive conversion to the expected reduced diketide (Siskos et al., 2005). To determine if our construct was active, it was incubated with a similar diketide mixture (Figure 4A). The polyketide chain used is one carbon shorter, representative of the diketide presented to this KR when the loading didomain (LDD) is primed by an acetyl group rather than a propionyl group (Kao et al., 1994). Most of the substrate was reduced to the expected product, and it had the same mass and retention time as an authentic sample (G. Liu, personal communication). However, ~3% of the product possessed an alternate stereochemistry.

At least four of the chiral centers of 6-dEB are controlled by the KRs of the erythromycin synthase. The first KR catalyzes a reduction that results in the hydroxyl group having an "R" stereochemistry, while the second, fifth, and sixth KRs catalyze the "S" reaction (quotation marks are used because lowest priority is given to the γ-carbon of the growing polyketide, a deviation from the RS system). From a sequence alignment of KRs that catalyze opposite reactions, an aspartate has been identified that is conserved in KRs that catalyze the "R" reduction (D1758 in the first KR) (Reid et al., 2003). The structure of the first KR suggests that F1801 might also help specify the "R" reduction.

To determine the importance of each of these residues, the single mutant D1758A and the double mutant D1758A/F1801G were assayed in the context of a model synthase (Figure 4B). The engineered synthase composed of the loading didomain and module 1 on one protein and module 2 and TE on another can synthesize a triketide lactone (TKL) in vivo (Menzella et al., 2005). Both the D1758A and D1758A/F1801G mutants are capable of producing the "natural" TKL, albeit at reduced titers compared to the unmutated synthase (~40% and ~10%). The identity of the "natural" TKL was confirmed through nuclear magnetic resonance spectroscopy; its spectrum matched a previous report (Kao et al., 1994). The mutants did not produce any novel TKLs, as judged by liquid chromatography/mass spectrometry.

Oligomerization States

Some or all of the β-carbon processing enzymes are hypothesized not to make contact through the 2-fold axis of the module in the head-to-head, tail-to-tail model (Staunton et al., 1996). The KR structure reported here

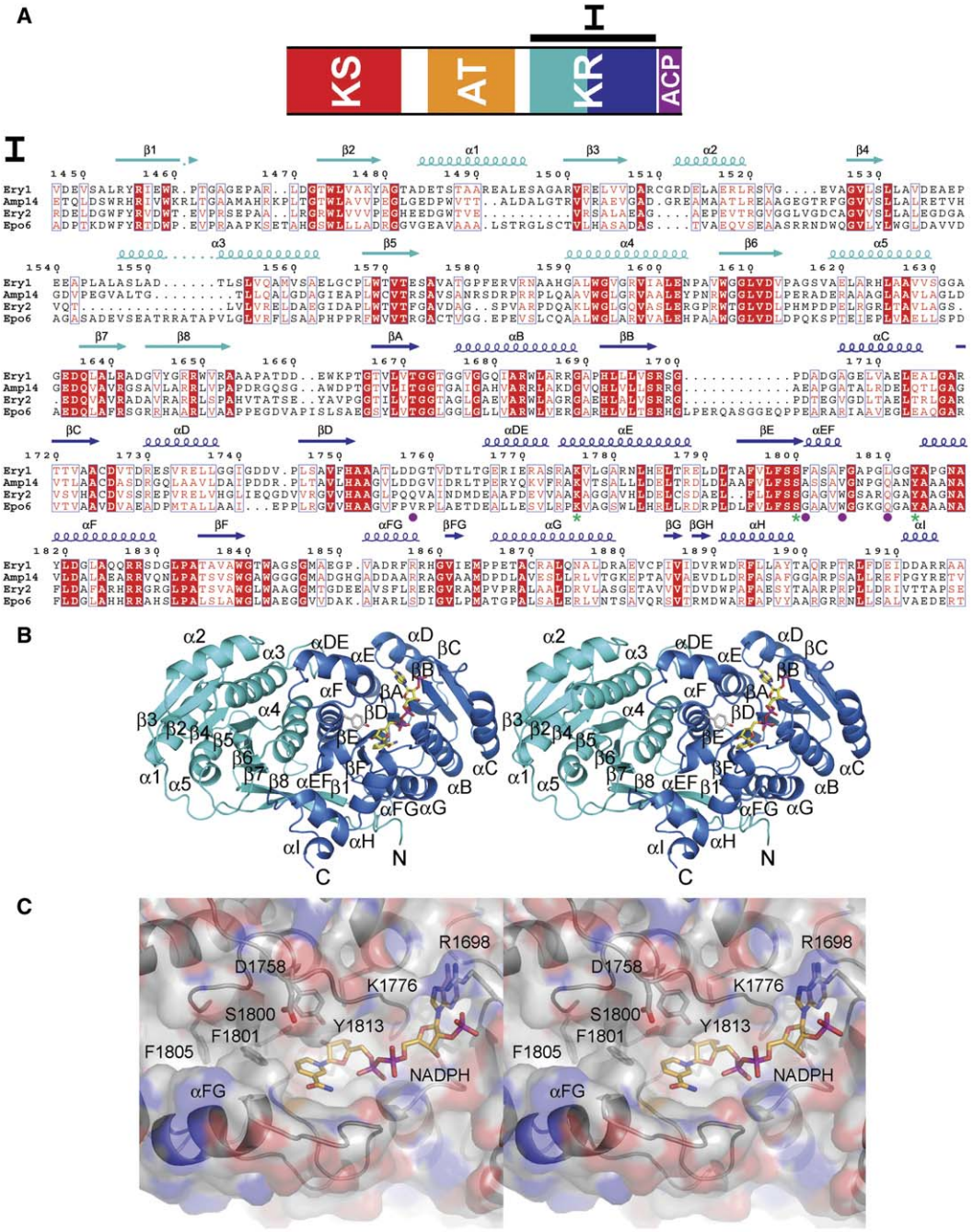

Figure 2. KR Alignment and Structure

(A) The aligned KRs are from modules containing the same set of domains. The first two catalyze reductions resulting in an "R" stereochemistry; the latter two catalyze reductions resulting in an "S" stereochemistry. Secondary structure elements are indicated above the sequence as coils and arrows for helices and strands, respectively. Elements are colored light blue and dark blue for the structural and catalytic halves of KR, respectively. Catalytic residues are marked by asterisks, and residues that may confer stereospecificity are marked by circles. Sequences: 1st KR of the erythromycin synthase, the 14th KR of the amphotericin synthase, the 2nd KR of the erythromycin synthase, and the 6th KR of the epothilone synthase.

(B) A stereodiagram displays the secondary structural elements of KR. NADPH and the catalytic tyrosine are represented as sticks.

(C) A stereodiagram of the active site illustrates the groove where NADPH and the polyketide bind. The left side of the groove is occluded by F1801.

shows that the KR domain is monomeric; however, the ER fragment structure shows that the ER domain is dimeric (Gogos et al., 2003). To confirm that the β-carbon processing enzymes are dimeric, the region encoding DH, ER, and KR from the fourth module of the erythromycin synthase (DH+ER+KR) was cloned and expressed. Purified DH+ER+KR migrated at ~233 kDa by gel filtration, which corresponds well with the expected dimer mass of 222 kDa. By itself, KR migrates at ~57 kDa, consistent with it being a monomer (Figure S1).

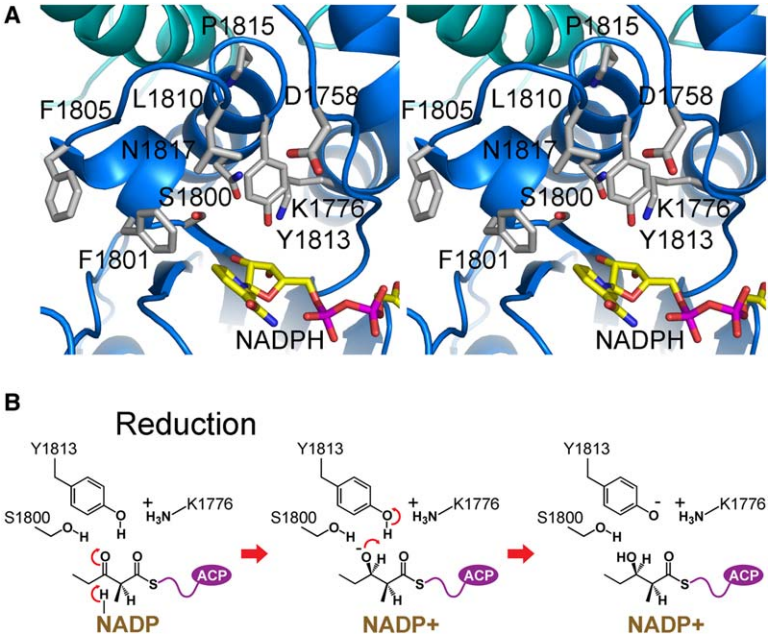

Figure 3. Chemistry of Reduction

(A) A stereodiagram of the active site shows the catalytic Y1813 and S1800, other key residues, and the NADPH nicotinamide (modeled, since no density was observed).

(B) Reduction catalyzed by the first KR. A diketide binds in the active site preloaded with NADPH. The β-carbonyl, bound by S1800 and Y1813, is attacked by the NADPH hydride from below. The oxygen accepts a proton from Y1813, resulting in a β-hydroxyl group of "R" stereochemistry.

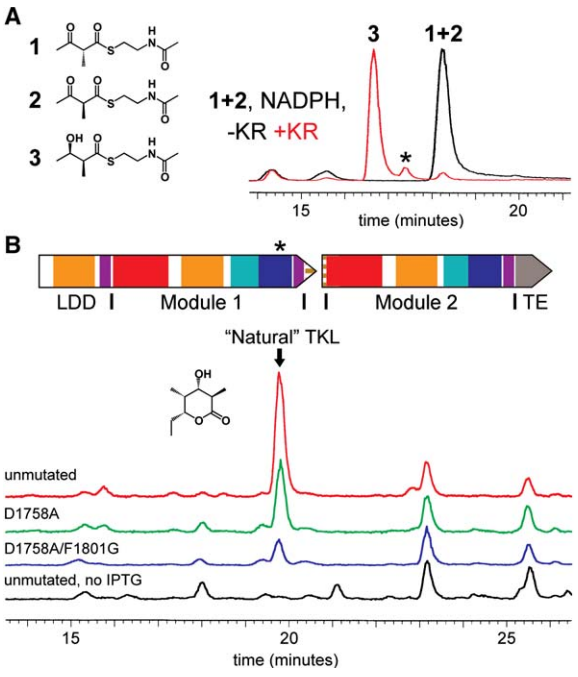

Figure 4. Functional Assays

(A) The isolated KR domain catalyzes the reduction of a diketide mixture, as shown by LC/MS ion count traces. The small peak between **1+2** and **3** (indicated by an asterisk) has the same mass as **3** and is probably a stereoisomer.

(B) Representative LC/MS ion count traces of culture extract from *E. coli* K207-3 expressing engineered triketide lactone synthases. The top trace shows compounds produced by cells containing the unmutated synthase. The bottom trace shows the background when IPTG is not added and the synthase is not expressed. Synthases with mutations to residues in the first KR domain (indicated by an asterisk) hypothesized to help control the stereochemistry of reduction still produce the natural TKL, albeit at lower titers compared to the unmutated synthase (~40% for D1758A; ~10% for D1758A/F1801G).

Domain Boundaries

A sequence analysis of a module containing an ER suggests that the structural and catalytic halves of KR form individual domains separated by an ER domain. The KR structure reported here reveals that the structural and catalytic subdomains are intimately associated. By mapping our structure onto the predicted secondary structure of the fourth module of the erythromycin synthase, which contains all of the β-carbon processing enzymes, the boundaries of KR and the neighboring domains could be more clearly defined (Figure 5A).

The boundaries of DH have not been adjusted since the erythromycin synthase was sequenced and annotated (Donadio and Katz, 1992). Using the former DH boundaries, ~120 residues lie between DH and β1 of the structural half of KR. This region is predicted by the program 3D-PSSM to contain four consecutive long β-strands, indicative of the hotdog fold in hydratases and dehydratases (Kelley et al., 2000). However, the catalytic residues of DH lie within the former boundaries of DH, which is also predicted to contain four consecutive long β-strands. When the sequence containing both putative hotdog folds was put into 3D-PSSM for fold recognition, thioesterase II was returned as a match. This enzyme contains the recently discovered double hotdog fold (Li et al., 2000). Alignments between modules with and without DH also suggest that DH is comprised of both regions.

ER is a reductase in the medium-chain dehydrogenase/reductase (MDR) family, as shown through sequence homology and partial crystal structure, and it is best structurally represented by quinone oxidoreductase (Gogos et al., 2003; Thorn et al., 1995; Edwards et al., 1996). The KR structure reveals that when ER is present, it is positioned between the two KR subdomains. Less than 15 residues separate the last β-strand of the structural subdomain of KR from the first β-strand of ER, and only 10 residues separate the last β-strand of

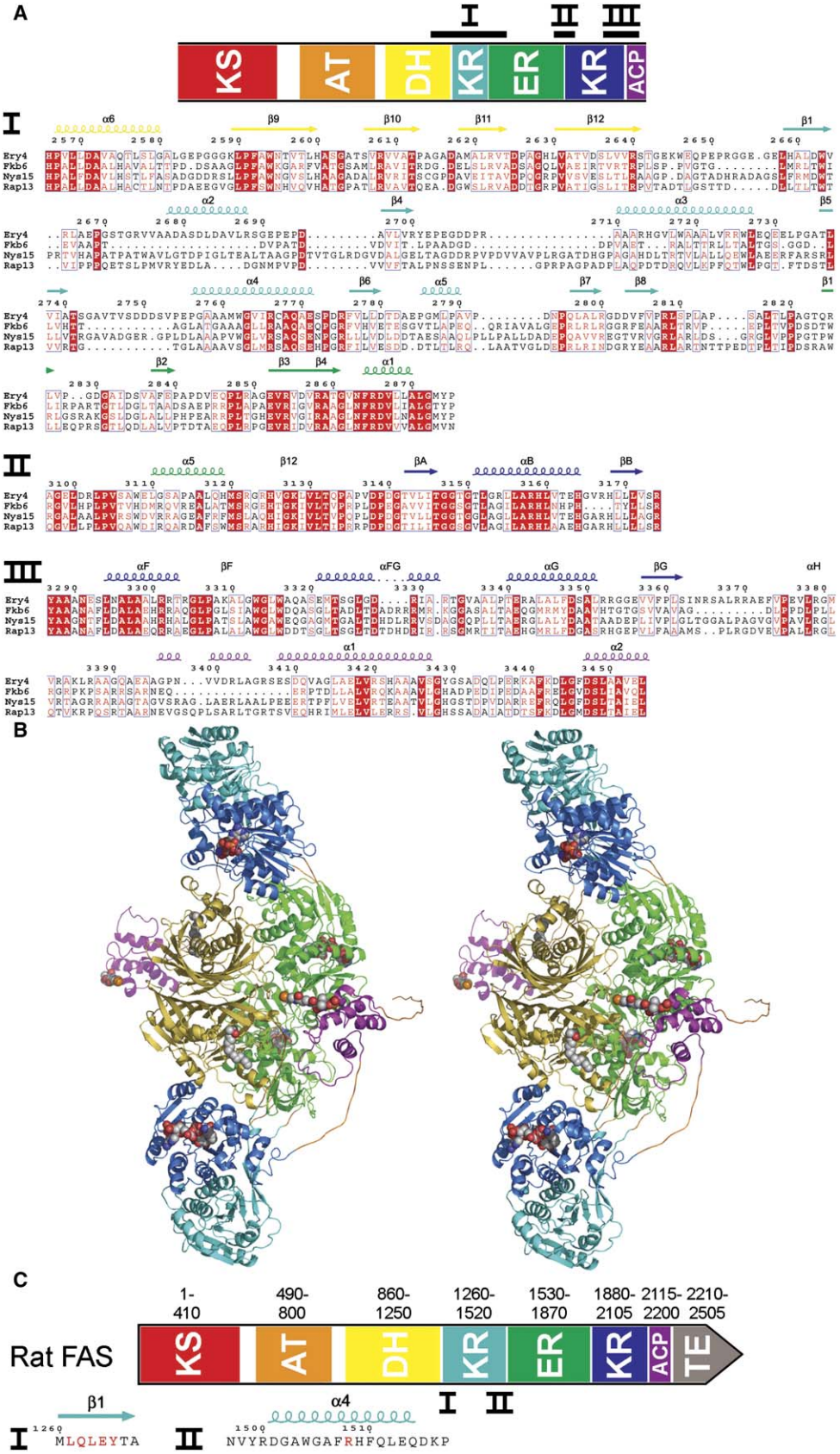

Figure 5. Domain Boundaries and Organization

(A) Complete modules from diverse synthases are aligned to display domain boundaries. The secondary structure, depicted by coils and arrows above the aligned sequences, was predicted by the program 3D-PSSM, and the secondary structure labels indicate where elements are

ER from the first β-strand of the catalytic subdomain of KR.

The regions N- and C-terminal to ACP are long, unconserved, and rarely contain large hydrophobic residues. It is unclear how many residues separate the end of KR from the first helix of ACP since αH is difficult to identify by sequence analysis. In a complete module, ~18 residues separate the last helix of ACP from the first β-strand of the following KS.

Quaternary Structure

A sequence alignment of KRs from modules that contain a DH with KRs from modules that do not contain a DH reveals differences between αB, αFG, and αG (Figure S2). The residues in and around these helices are much more highly conserved in KRs from modules with a DH. The conservation in αFG is especially surprising since it makes few contacts with the rest of KR. Since these helices are clustered on the same region of KR, they may represent an interaction surface that makes contact with DH.

We deduced the relative positions of the β-carbon processing enzymes and ACP in a complete module by arranging representative structures of each enzyme domain subject to the constraints of domain termini locations, interdomain linker length, and the proposed DH interface (Figure 5B). Thioesterase II (PDB code: 1C8U) was used for DH (Li et al., 2000), quinone oxidoreductase (PDB code: 1QOR) was used for ER (Thorn et al., 1995), our structure was used for KR, and actinorhodin ACP (PDB code: 2AF8) was used for ACP (Crump et al., 1997). The domains were positioned by using Quanta (Accelrys). First, the 2-fold axis of the ER dimer observed in the ER fragment (and in all structures of MDR reductases) was used as the 2-fold axis of the module. Since ER is inserted into the loop between β8 and βA of KR, the N- and C-termini of ER were fused to the ends of this opened loop, constraining the position of KR relative to ER. Next, the DH dimer was placed on the 2-fold axis so that its C-termini were near the N-termini of each KR monomer, and so that its surface contacted αB, αFG, and αG of KR. Finally, ACP was positioned near the C-terminus of KR since it starts ~15 residues after the KR ends.

Discussion

Reduction

KR controls the stereochemistry of the β-hydroxyl group of a polyketide (Figure 3). It is hypothesized that the stereochemistry is determined by the direction that the polyketide enters the active site (Reid et al., 2003; Caffrey, 2005). KRs that perform the reduction leading to an "R" stereochemistry possess an aspartate on one side of the active site groove. KRs that catalyze an "S" stereochemistry lack this aspartate but usually possess a tryptophan on the opposite side of the groove (replacing F1805). One might speculate that residues on nearby αFG help in conferring stereospecificity since they may clamp down on a polyketide when it is bound in the groove; however, residues on the corresponding helix of the related tropinone reductase were shown not to influence specificity to a large extent (Figure 2C) (Nakajima et al., 1999). Enzymology of isolated KR domains with substrate analogs has revealed that neither the phosphopantetheinyl arm nor ACP is needed to determine the stereochemistry of reduction (Siskos et al., 2005).

In the related enzyme FabG, the aspartate hydrogen bonds to a conserved glutamine 3 residues N-terminal to the catalytic tyrosine, apparently orienting its NH_2 group to contact the thioester carbonyl of the substrate (Figure 6A). This glutamine is highly conserved in KRs, including those that catalyze the "S" reaction. The aspartate is absent in KRs that catalyze the "S" reaction, and the glutamine may be oriented by the neighboring backbone (Figure 6B). We hypothesize that the tryptophan conserved in these enzymes may help structure the backbone for this interaction. The glutamine NH_2 may still hydrogen bond to the substrate thioester carbonyl, guiding polyketides into the groove from the left side.

The first KR of the erythromycin synthase is highly specialized. If the aspartate (D1758) helps it specify an "R" stereochemistry, how it does so is not obvious. The conserved glutamine is replaced by a leucine (L1810) and cannot direct the polyketide to either side of the groove (Figure 3A). However, F1801 on the left side of the groove may both sterically block the "S" reaction and encourage the "R" reaction through hydrophobic contacts with the diketide substrate.

To determine the importance of D1758, it was mutated to an alanine in the context of an engineered synthase (Figure 4B). The KR was not severely compromised, as the synthase was able to produce the expected "natural" TKL at ~40% the titer of the unmutated synthase. If the KR had lost its stereoselectivity, TKL stereoisomers might be expected, according to a recent study of hybrid TKL synthases (Menzella et al., 2005). None were observed. We hypothesized that F1801 is the principal determinant of stereospecificity, yet the double mutant D1758A/F1801G still produced the natural "TKL" at ~10% the titer of the unmutated synthase and no TKL stereoisomers were observed. To determine which residues control the stereospecificity of reduction, site-directed mutagenesis like that performed on tropinone reductase will need to be conducted on isolated KR domains, eliminating the complications that arise from "gate-keeping" that may be performed by downstream enzymes. Appropriate substrate analogs should be used since recent KR enzymology and our enzymology of isolated KR domains indicate that imperfect analogs can be reduced incorrectly (Figure 4A) (Siskos et al., 2005).

When a polyketide binds to a KR, it must lie on top of the nicotinamide ring of NADPH in order for the pro-S hydride to attack the β-carbonyl (McPherson et al., 1998). Thus, for catalysis to occur, NADPH must bind to

expected based on sequence alignments with proteins of known structure. Sequences: the 4th module of the erythromycin synthase, the 6th module of the ascomycin synthase, the 15th module of the nystatin synthase, and the 13th module of the rapamycin synthase.

(B) A stereodiagram of DH, ER, KR, and ACP shows how they may be arranged in a complete module. Polyglycine linkers, in orange, were built to connect the domains. The molecules bound to DH are LDAO (they were in the active site of thioesterase II), and those bound to ER and KR are NADPH. The phophopantetheine arm of ACP is also displayed.

(C) Domain boundaries learned from PKS β-carbon processing enzymes applied to the *Rattus norvegicus* FAS. The sequence LQLEY marks the beginning of the KR structural subdomain. Mutagenesis of α4, including point mutants of R1508, abolished KR and ER function.

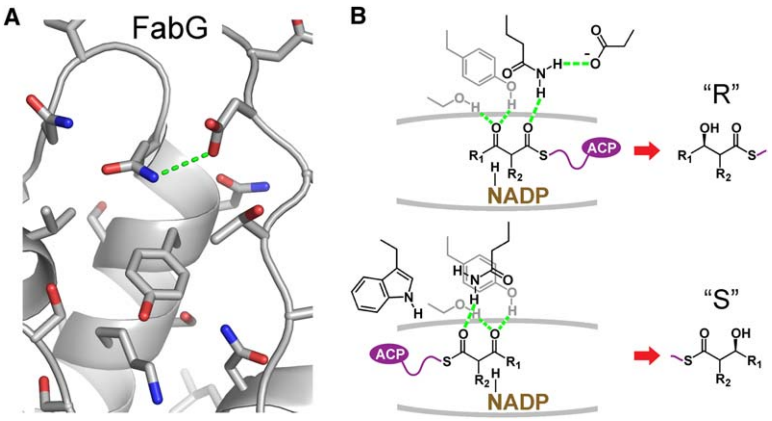

Figure 6. Control of Stereochemistry

(A) In the related fatty acid synthase enzyme, FabG (PDB code: 2C07), the aspartate orients the glutamine.

(B) Stereochemistry may be controlled in part by the NH_2 group of a conserved glutamine that can donate a hydrogen bond to the substrate thioester carbonyl. In enzymes that catalyze an "R" reduction, a conserved aspartate may orient the glutamine NH_2 so that a polyketide enters from the right side of the groove. In enzymes catalyzing the "S" reaction, a tryptophan on the left side of the groove may help orient the glutamine NH_2 so that the polyketide enters from that side.

the protein before the polyketide. Well-diffracting crystals of KR could not be grown in the absence of NADPH, suggesting that the cofactor orders the enzyme for catalysis as it does in FabG (Price et al., 2004).

Epimerization

The first and third modules of the erythromycin synthase catalyze epimerizations of the α-methyl group, although the enzyme that performs this reaction has not been determined (Weissman et al., 1997; Caffrey, 2005). There are several reasons to believe that KR doubles as an epimerase even though no SDR enzyme is known to catalyze a similar reaction: (1) No module lacking a KR has been observed to catalyze an epimerization. (2) A module that contains a reductase-incompetent KR, but no other β-carbon processing enzyme, can catalyze epimerization. (3) Furthermore, the tyrosine that is catalytic in reductase-competent KRs is still conserved in these KRs. The epimerase activity must be independent of NADPH since the nucleotide binding motif of the KR from the third module of the erythromycin synthase is absent.

Alignments of KRs from epimerization-catalyzing modules that do not contain other β-carbon processing enzymes implicate the active site tyrosine in the abstraction of the acidic hydrogen on the polyketide α-carbon (Figure 7). After the subsequent enolization, the polyketide may exit the active site and tautomerize to one of two keto forms, one being the epimerized polyketide. The nonproductive tautomerization yields the original substrate that can be accepted by KR until it is epimerized. The catalytic tyrosines of other solved SDR structures reside within αF; however, Y1813 from the KR of the first module of the erythromycin synthase lies outside this helix and may have sufficient mobility to access the acidic polyketide hydrogen. Y1813 is apparently liberated by the helix-breaking P1815. Its average temperature factor is twice that of N1817, one turn into αF (34 A^3 versus 17 A^3) (Figure 7B). In the third KR of the erythromycin synthase, the asparagine corresponding to N1817 is replaced by a serine. To compensate for the missing asparagine side chain, αF may need to partially unravel, again liberating the tyrosine for the epimerization reaction. In nonepimerizing KRs, a more ordered αF probably prevents the tyrosine from accessing the acidic polyketide hydrogen (Figure 7C). Intriguingly, DHs may also catalyze epimerization, since, in some modules known to catalyze epimerization (such as the fourth module of the ascomycin synthase or the sixth module of the rapamycin synthase), the KR tyrosine is absent but a supposedly inactive DH is present. This reaction is easier to understand than KR-catalyzed epimerization, as the first step catalyzed by a DH during dehydration is the abstraction of an α-carbon hydrogen.

Domain Organization

Outside of the module, the docking domains and TE are dimeric (Tsai et al., 2001, 2002; Broadhurst et al., 2003). However, it was unclear how many domains within the module would also be dimeric. If every enzyme within the module made contacts across the 2-fold axis, ACP would have to diffuse farther than the peptide linkers on each side would permit. The deduced quaternary structure of the β-carbon processing enzymes indicates a surprising amount of contact across the 2-fold axis. However, the structural half of KR enables the KR domain to be monomeric and loop out from the 2-fold axis, allowing DH and ER to come closer to each other. KS probably makes contact across the 2-fold axis since all known type II KSs (type II enzymes are functional as separate polypeptides; several of these structures have been solved) are dimeric and its active site lies at the dimer interface. However, AT may loop out since all known type II ATs are monomeric. There may be protein-protein contacts all along the 2-fold axis. A large number of inactive enzymes are present within modules, possibly indicating that they make important contacts.

The active sites of DH, ER, and KR are all accessible to ACP. Bound by peptide linkers on both ends, ACP can diffuse between each enzyme in the module as well as the next KS or TE, akin to the lipoyl domains and biotinyl domains of other multienzyme proteins (Perham, 2000). The linkers also prevent a polyketide from interacting with enzymes farther away in the synthase. However, a polyketide bound to the ACP of the third module of the epothilone synthase may have sufficient freedom to access DH of the fourth module (Tang et al., 2000). The ~18 Å phosphopantetheinyl arm contributes relatively little translational freedom to the polyketide compared to the peptide linkers on both ends of ACP.

Most SDR enzymes are either dimeric or tetrameric, and the principle interface is formed by helices αE and αF (Jornvall et al., 1995). The structural subdomain of KR contributes these important stabilizing interactions

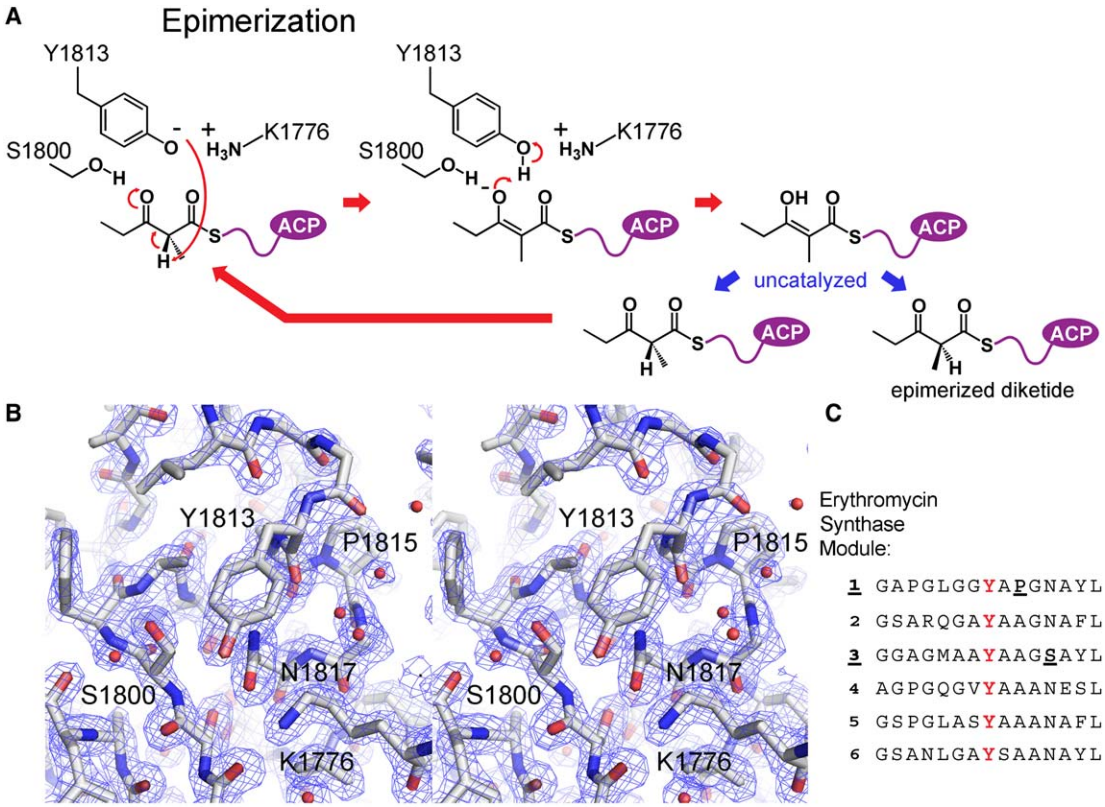

Figure 7. Epimerization

(A) Hypothesized mechanism of epimerization. The diketide formed by the first KS enters the active site of the first KR. The mobile Y1813 acts as a base, acquiring the acidic hydrogen of the diketide to form an enolate. The enolate oxygen accepts the proton back from Y1813, and the enolized diketide is released from the KR. An uncatalyzed tautomerization back to the keto form results in a mixture of the original diketide and the epimerized diketide. The original diketide can be accepted until it is epimerized.

(B) A stereodiagram of the KR active site displays the $2F_o - F_c$ electron density maps contoured at 1.5σ. P1815 breaks the helix that contains the catalytic tyrosine in related SDR enzymes, allowing it greater mobility. The temperature factors for Y1813 and neighboring residues are comparatively high.

(C) The sequence surrounding the catalytic tyrosine from each KR of the erythromycin synthase. The first and third modules catalyze epimerization. Residues that may allow the tyrosine sufficient freedom to catalyze epimerization are underlined.

to the catalytic subdomain through the interaction of α3 and α4 with αE and αF. In fungal MFE-2, two consecutive dehydrogenase domains are present—one that oxidizes short chains and one that oxidizes long chains. The fragment of *Candida tropicalis* MFE-2 containing these dehydrogenases was crystallized and found to be monomeric, indicating that the two dehydrogenase domains associate (Ylianttila et al., 2004). Perhaps KR evolved from such an enzyme, losing the catalytic, but not structural properties, of one domain.

If modular synthases evolved through the fusion of genes encoding type II enzymes, it is plausible that an ancestral type II ER inserted into the loop between the two subdomains of KR. The ER fold begins after β8 of the KR structural subdomain and ends before βA of the catalytic subdomain. The N- and C-termini of related MDR enzymes are near one another; thus, the ancestral insertion may have been relatively uncomplicated. The segment joining ER to the KR catalytic subdomain is more highly conserved in sequence and length than the segment joining it to the KR structural subdomain, possibly indicating that it helps fix the relative positions of the KR and ER domains. Similar domain insertions may have also occurred with AT and the rare methyltransferase domain (Tang et al., 2000; Cheng et al., 2003).

PKS Modules and FASs

It is hypothesized that modular PKSs evolved from FASs since a complete module contains the same domains in the same order. If so, they might share a similar three-dimensional organization. The animalian FAS has been shown to possess some conformational flexibility, but it is fairly rigid on the whole. Reconstructions of the human FAS from electron micrographs have been made at 16 Å resolution, and crystals have even been grown. The latest reconstructions show the head-to-head, tail-to-tail organization of the FAS domains through a long 2-fold axis (Asturias et al., 2005).

A ~520 residue region termed the "core" (residues ~1010–1530) precedes ER in the well-studied *Rattus norvegicus* FAS. It can be much shorter: the *Drosophila melanogaster* FAS core is ~380 residues. Mutagenesis performed on the C-terminal portion of the rat FAS core inactivated KR and ER (Witkowski et al., 2004). From the KR structure presented here, it is now clear that the

mutations were of α4 in the structural subdomain of KR, a helix that provides many stabilizing contacts to the catalytic subdomain (Figure 5C). Without these interactions, the structural and catalytic subdomains of KR could dissociate, conceivably destabilizing ER in the process since it is positioned between them. The sequence identifying the β-strand β1, which begins the structural subdomain, is more subtle than in PKSs, appearing as 2 large hydrophobic residues separated by 3 variable residues; it is LQLEY in *R. norvegicus*. It is probable that the sequence N-terminal to the structural half of KR is from the second hotdog fold of DH. Thus, the core probably consists of the C-terminal half of DH and the N-terminal half of KR.

The KR structure suggests catalytic similarities between PKS and FAS enzymes even at the stereochemical level. The KRs from complete modules possess the aspartate, but not the tryptophan, in the active site groove (Figure 6B). This pattern is indicative of the "R" reduction, suggesting that DH only accepts a β-hydroxyl group of this stereochemistry. FAS KRs also possess the aspartate, but not tryptophan, and are known to catalyze the "R" stereochemistry (Smith et al., 2003). The FAS DH accepts the resulting "R" product. The glutamine hypothesized to guide substrates into the KR active site groove is also conserved in FAS KRs. Finally, the mysterious swapping of the asparagine and lysine positions, compared to other SDR enzymes, also occurs in FAS KRs.

The KR structure may also hint at the origin of the FAS KR. On several levels, the KR domain shows similarities to an enzyme from a β-oxidation pathway, the dehydrogenase of MFE-2. This enzyme catalyzes virtually the same reaction as KR. Its substrate is a (3R)-hydroxyacyl chain (the product of a neighboring hydratase that possesses the double hotdog fold hypothesized for DH). Thus, the hydroxyl group of its reactant is of the same stereochemistry as the hydroxyl group of the product from a KR in a complete module or FAS. The dehydrogenase of MFE-2 is unique in β-oxidation pathways in that it can oxidize branched fatty acids (acyl chains with an α-substituent, commonplace in polyketides). These catalytic similarities and the structural homology of these enzymes suggest an evolutionary link.

The precise boundaries between the β-carbon processing domains will be valuable in the design of hybrid synthases since they detail how domains can be swapped more cleanly. In time, structural and engineering studies will elucidate how substrate specificity and stereochemistry are controlled by these enzymes, enabling the synthesis of designer polyketides.

Experimental Procedures

Cloning

The DNA encoding T2, from S1444 to R1925, was PCRed from synthetic *eryAI* with primers 5′-GGAGATATACATATGTCTACCGAGGT TGATGAAGTC-3′ and 5′-GTGGTGCTCGAGTCATCAGCGTGGCTC AGCAGCGGCCTGC-3′, cut with NdeI and XhoI, and ligated into pET28b. The DNA encoding DH+ER+KR, from H2362 to S3409, was PCRed from synthetic *eryAII* with primers 5′-GGAGATATACATATG CACCGCCCAGCAGATGTTAGC-3′ and 5′-GTGGTGCTCGAGTCAT CACGATTCGCTACGACCGGCTAAG-3′, cut with NdeI and XhoI, and ligated into pET28b (Kodumal et al., 2004).

Expression and Purification

BL21(DE3) cells transformed with either the plasmid encoding KR or DH+ER+KR were grown in LB with 20 mg/l kanamycin at 37°C until they reached 0.4 OD_{600}. They were induced with 1 mM IPTG and grown for 40 hr at 18°C. Cells were spun down and resuspended in 40 mM HEPES (pH 7.0), 0.5 M NaCl, 5 mM β-ME, and 1 μM PMSF, sonicated, and spun down at 30,000 × g for 30 min. The supernatant was poured over a nickel-NTA column, washed with 25 mM imidazole (in lysis buffer), and the protein was eluted with 250 mM imidazole. The protein was exchanged into gel filtration buffer (10 mM HEPES, 150 mM NaCl, 1 mM DTT [pH 7.0]), and thrombin was added to cleave off the histidine tag at 21°C for 1 hr. Thrombin was removed by a benzamidine sepharose column, and the protein mixture was concentrated and run through a Sephadex 200 gel filtration column. Selenomethionine-incorporated KR was expressed in BL21(DE3) cells in M9 (4 g/l glucose, 6 g/l Na_2HPO_4, 3 g/l KH_2PO_4, 1 g/l NH_4Cl, 0.5 g/l NaCl, 1 mM $MgSO_4$, 0.1 mM $CaCl_2$) minimal media with 20 mg/l kanamycin. After growing to 0.4 OD_{600} at 37°C, they were supplied with lysine, phenylalanine, and threonine, each at 100 mg/l; isoleucine, leucine, and valine, each at 50 mg/l; and selenomethionine at 60 mg/l. After 15 min, they were induced with 1 mM IPTG and grown for 40 hr at 18°C. The purification was the same as for the native protein.

Gel Filtration

A Sephadex 200 gel filtration column was equilibrated with gel filtration buffer and injected with 0.5 ml samples. The KR and DH+ER+KR fragments were compared to known standards. Dextran blue 2000 and tyrosine were used to determine V_o and V_t, respectively. $K_{av} = (V_e - V_o)/(V_t - V_o)$, where V_e is the volume at which the protein elutes.

Crystallization and Data Collection

The T2 fragment was concentrated to 3 mg/ml in gel filtration buffer and crystallized by hanging drop vapor diffusion in 35% PEG3350, 0.2 M guanidinium hydrochloride, 0.1 M HEPES (pH 7.0). Crystals grew to full size (200 × 100 × 50 μm) in 1 week. Two crystal forms were present in the drop and often grew together in twinned crystals, and surgery was often needed to separate them. Crystals were frozen in mother liquor in the nitrogen stream. Data were collected at the ALS Beamline 8.3.1.

Data Processing and Refinement

ELVES processed the anomalous dispersion data (Holton and Alber, 2004). The selenium sites were located, and phases were generated by using CNS (Brunger et al., 1998). A model was built with Quanta for 60% of the protein before it was used to generate phases. The rest of the model was created through multiple rounds of building and refining in CNS.

Isolated KR Domain Assay

Analagous to a recent study, reactions were incubated in 100 μl in 400 mM NaH_2PO_4 (pH 7.5) for 16 hr at 22°C, by using 10 mM NADPH, 3 mM unreduced diketide analog (G. Liu, personal communication), and 1 μM isolated KR domain (Siskos et al., 2005). The reaction was extracted with 1 ml ethyl acetate. The extract was separated by a 0%–30% acetonitrile/water (0.1% TFA) gradient on a C_{18} reverse-phase column and analyzed by the ion count trace from a connected mass spectrometer. The products were compared to authentic standards (G. Liu, personal communication).

Triketide Lactone Synthase Assay

The loading didomain and module 1 were cloned between the NdeI and EcoRI sites of pET21, module 2 and TE were cloned between the NdeI and EcoRI sites of pET28, and both plasmids were transformed into *E. coli* K207-3 (Menzella et al., 2005). The D1758A mutant was engineered by using the Quickchange protocol (Stratagene) with primers 5′-GGCGGCAACCTTGGATGCCGGCACCGTCGATAC TC-3′ and 5′-GAGTATCGACGGTGCCGGCATCCAAGGTTGCCG CC-3′. The D1758A/F1801G double mutant was engineered by using the Quickchange protocol on the D1758A plasmid with primers 5′-CG TGCTGTTTTCCAGTGGTGCGTCGGCCTTTGGTG-3′ and 5′-CACCA AAGGCCGACGCACCACTGGAAAACAGCACG-3′. A starter culture was grown overnight in LB at 37°C, was used to inoculate 1 l M9 minimal media supplied with 1 mM β-alanine, 50 mg/l carbenecillin, and

20 mg/l kanamycin, and was grown at 37ºC until the OD_{600} reached 0.5. The temperature was decreased to 20ºC, and cells were induced with 1 mM IPTG; media were supplemented with 50 mM glutamate (pH 7.0), 50 mM succinate (pH 7.0), and 50 mM propionate (pH 7.0). After 3 days, cells were spun down, and the supernatant was acidified to pH 1.5 with phosphoric acid and extracted twice with methylene chloride. Methylene choride was evaporated, and the extract was separated by a 20%–30% acetonitrile/water (0.1% TFA) gradient on a C_{18} reverse-phase column. Fractions were analyzed by mass spectrometry and nuclear magnetic resonance spectroscopy.

Supplemental Data

Supplemental Data including Figures S1 and S2 are available at http://www.structure.org/cgi/content/full/14/4/737/DC1/.

Acknowledgments

We thank Daniel Santi for supplying the synthetic polyketide synthase genes, Ralph Reid for his help in analyzing KR enzymology and domain boundaries, Hugo Menzella and Sunil Chandran for help with the triketide lactone assay, Gary Liu for providing the diketide analogs, and Janet Finer-Moore for help in crystallography and interpreting experimental data. Research was supported by the National Cancer Institute National Institutes of Health (NIH) grant CA63081 and Training Grant #5 T32 CA090270.

Received: November 1, 2005
Revised: January 11, 2006
Accepted: January 17, 2006
Published online: March 15, 2006

References

Aparicio, J.F., Caffrey, P., Marsden, A.F., Staunton, J., and Leadlay, P.F. (1994). Limited proteolysis and active-site studies of the first multienzyme component of the erythromycin-producing polyketide synthase. J. Biol. Chem. *269*, 8524–8528.

Asturias, F.J., Chadick, J.Z., Cheung, I.K., Stark, H., Witkowski, A., Joshi, A.K., and Smith, S. (2005). Structure and molecular organization of mammalian fatty acid synthase. Nat. Struct. Mol. Biol. *12*, 225–232.

Bedford, D., Jacobsen, J.R., Luo, G., Cane, D.E., and Khosla, C. (1996). A functional chimeric modular polyketide synthase generated via domain replacement. Chem. Biol. *3*, 827–831.

Broadhurst, R.W., Nietlispach, D., Wheatcroft, M.P., Leadlay, P.F., and Weissman, K.J. (2003). The structure of docking domains in modular polyketide synthases. Chem. Biol. *10*, 723–731.

Brunger, A.T., Adams, P.D., Clore, G.M., DeLano, W.L., Gros, P., Gross-Kunstleve, R.W., Jiang, J.S., Kuszewski, J., Nilges, M., Pannu, N.S., et al. (1998). Crystallography & NMR system: a new software suite for macromolecular structure determination. Acta Crystallogr. D Biol. Crystallogr. *54*, 905–921.

Caffrey, P. (2005). The stereochemistry of ketoreduction. Chem. Biol. *12*, 1060–1062.

Cheng, Y.Q., Tang, G.L., and Shen, B. (2003). Type I polyketide synthase requiring a discrete acyltransferase for polyketide biosynthesis. Proc. Natl. Acad. Sci. USA *100*, 3149–3154.

Crump, M.P., Crosby, J., Dempsey, C.E., Parkinson, J.A., Murray, M., Hopwood, D.A., and Simpson, T.J. (1997). Solution structure of the actinorhodin polyketide synthase acyl carrier protein from *Streptomyces coelicolor* A3(2). Biochemistry *36*, 6000–6008.

Donadio, S., and Katz, L. (1992). Organization of the enzymatic domains in the multifunctional polyketide synthase involved in erythromycin formation in *Saccharopolyspora erythraea*. Gene *111*, 51–60.

Edwards, K.J., Barton, J.D., Rossjohn, J., Thorn, J.M., Taylor, G.L., and Ollis, D.L. (1996). Structural and sequence comparisons of quinone oxidoreductase, zeta-crystallin, and glucose and alcohol dehydrogenases. Arch. Biochem. Biophys. *328*, 173–183.

Gogos, A., Mu, H., and Shapiro, L. (2003). Putative enoyl reductase domain of a polyketide synthase. 1PQW (see http://www.rcsb.org/pdb/navbarsearch.do?newSearch=yes&isAuthorSearch=no&radioset=All&inputQuickSearch=1pqw&image.x=42&image.y=5).

Haapalainen, A.M., Koski, M.K., Qin, Y.M., Hiltunen, J.K., and Glumoff, T. (2003). Binary structure of the two-domain (3R)-hydroxyacyl-CoA dehydrogenase from rat peroxisomal multifunctional enzyme type 2 at 2.38 Å resolution. Structure (Camb) *11*, 87–97.

Holm, L., and Sander, C. (1996). Mapping the protein universe. Science *273*, 595–603.

Holton, J., and Alber, T. (2004). Automated protein crystal structure determination using ELVES. Proc. Natl. Acad. Sci. USA *101*, 1537–1542.

Jornvall, H., Persson, B., Krook, M., Atrian, S., Gonzalez-Duarte, R., Jeffrey, J., and Ghosh, D. (1995). Short-chain dehydrogenases/reductases (SDR). Biochemistry *34*, 6003–6013.

Kao, C.M., Luo, G., Katz, L., Cane, D.E., and Khosla, C. (1994). Engineered biosynthesis of a triketide lactone from an incomplete modular polyketide synthase. J. Am. Chem. Soc. *116*, 11612–11613.

Kelley, L.A., MacCallum, R.M., and Sternberg, M.T. (2000). Enhanced genome annotation using structural profiles in the program 3D-PSSM. J. Mol. Biol. *299*, 499–520.

Kodumal, S.J., Patel, K.G., Reid, R., Menzella, H.G., Welch, M., and Santi, D.V. (2004). Total synthesis of long DNA sequences: synthesis of a contiguous 32-kb polyketide synthase gene cluster. Proc. Natl. Acad. Sci. USA *101*, 15573–15578.

Li, J., Derewenda, U., Dauter, Z., Smith, S., and Derewenda, Z.S. (2000). Crystal structure of the *Escherichia coli* thioesterase II, a homolog of the human Nef binding enzyme. Nat. Struct. Biol. *7*, 555–559.

McDaniel, R., Kao, C.M., Hwang, S.J., and Khosla, C. (1997). Engineered intermodular and intramodular polyketide synthase fusions. Chem. Biol. *4*, 667–674.

McPherson, M., Khosla, C., and Cane, D.E. (1998). Erythromycin biosynthesis: the β-ketoreductase domains catalyze the stereospecific transfer of the 4-pro-S hydride of NADPH. J. Am. Chem. Soc. *120*, 3267–3268.

Menzella, H.G., Reid, R., Carney, J.R., Chandran, S.S., Reisinger, S.J., Patel, K.G., Hopwood, D.A., and Santi, D.V. (2005). Combinatorial polyketide biosynthesis by de novo design and rearrangement of modular polyketide synthase genes. Nat. Biotechnol. *23*, 1171–1176.

Nakajima, K., Kato, H., Oda, J., Yamada, Y., and Hashimoto, T. (1999). Site-directed mutagenesis of putative substrate-binding residues reveals a mechanism controlling the different stereospecificities of two tropinone reductases. J. Biol. Chem. *274*, 16563–16568.

O'Hagan, D.O. (1991). The Polyketide Metabolites (Chichester, UK: Ellis Horwood).

Oppermann, U., Filling, C., Hult, M., Shafqat, N., Wu, X., Lindh, M., Shafqat, J., Nordling, E., Kalberg, Y., Persson, B., et al. (2003). Short-chain dehydrogenases/reductases (SDR): the 2002 update. Chem. Biol. Interact. *143–144*, 247–253.

Perham, R.N. (2000). Swinging arms and swinging domains in multifunctional enzymes: catalytic machines for multistep reactions. Annu. Rev. Biochem. *69*, 961–1004.

Price, A.C., Zhang, Y.M., Rock, C.O., and White, S.W. (2004). Cofactor-induced conformational rearrangements establish a catalytically competent active site and a proton relay conduit in FabG. Structure (Camb) *12*, 417–428.

Reid, R., Piagentini, M., Rodriguez, E., Ashley, G., Viswanathan, N., Carney, J., Santi, D.V., Hutchinson, C.R., and McDaniel, R. (2003). A model of structure and catalysis for ketoreductase domains in modular polyketide synthases. Biochemistry *42*, 72–79.

Ruan, X., Pereda, A., Stassi, D., Zeidner, D., Summers, R.G., Jackson, M., Shivakumar, A., Kakavas, S., Staver, M.J., Donadio, S., et al. (1997). Acyltransferase domain substitutions in erythromycin polyketide synthase yield novel erythromycin derivatives. J. Bacteriol. *179*, 6416–6425.

Siskos, A.P., Baerga-Ortiz, A., Bali, S., Stein, V., Mamdani, H., Spiteller, D., Popovic, B., Spencer, J.B., Staunton, J., Weissman, K.J., et al. (2005). Molecular basis of Celmer's rules: stereochemistry of catalysis by isolated ketoreductase domains from modular polyketide synthases. Chem. Biol. *12*, 1145–1153.

Smith, S., Witkowski, A., and Joshi, A.K. (2003). Structural and functional organization of the animal fatty acid synthase. Prog. Lipid Res. *42*, 289–317.

Staunton, J., and Weissman, K.J. (2001). Polyketide biosynthesis: a millennium review. Nat. Prod. Rep. *18*, 380–416.

Staunton, J., and Wilkinson, B. (1997). Biosynthesis of erythromycin and rapamycin. Chem. Rev. *97*, 2611–2630.

Staunton, J., Caffrey, P., Aparicio, J.F., Roberts, G.A., Bethell, S.S., and Leadlay, P.F. (1996). Evidence for a double-helical structure for modular polyketide synthases. Nat. Struct. Biol. *3*, 188–192.

Tang, L., Shah, S., Chung, L., Shah, S., Chung, L., Carney, J., Katz, L., Khosla, C., and Julien, B. (2000). Cloning and heterologous expression of the epothilone gene cluster. Science *287*, 640–642.

Thorn, J.M., Barton, J.D., Dixon, N.E., Ollis, D.L., and Edwards, K.J. (1995). Crystal structure of *Escherichia coli* QOR quinone oxidoreductase complexed with NADPH. J. Mol. Biol. *249*, 785–799.

Tsai, S.C., Miercke, L.J., Krucinski, J., Gokhale, R., Chen, J.C., Foster, P.G., Cane, D.E., Khosla, C., and Stroud, R.M. (2001). Crystal structure of the macrocycle-forming thioesterase domain of the erythromycin polyketide synthase: versatility from a unique substrate channel. Proc. Natl. Acad. Sci. USA *98*, 14808–14813.

Tsai, S.C., Lu, H., Reid, D.E., Khosla, C., and Stroud, R.M. (2002). Insights into channel architecture and substrate specificity from crystal structures of two macrocycle-forming thioesterases of modular polyketide synthases. Biochemistry *41*, 12598–12606.

Weissman, K.J., Timoney, M., Bycroft, M., Grice, P., Hanefeld, U., Staunton, J., and Leadlay, P.F. (1997). The molecular basis of Celmers rules: the stereochemistry of the condensation step in chain extension on the erythromycin polyketide synthase. Biochemistry *36*, 13849–13855.

Witkowski, A., Joshi, A.K., and Smith, S. (2004). Characterization of the β-carbon processing reactions of the mammalian cytosolic fatty acid synthase: role of the central core. Biochemistry *43*, 10458–10466.

Ylianttila, M.S., Qin, Y.M., Hiltunen, J.K., Glumoff, T., et al. (2004). Site-directed mutagenesis to enable and improve crystallizability of *Candida tropicalis* (3R)-hydroxyacyl-CoA dehydrogenase. Biochem. Biophys. Res. Commun. *324*, 25–30.

Accession Numbers

The atomic coordinates have been deposited in the Protein Data Bank with accession codes 2FR0 and 2FR1 for the two crystal forms of KR and 2FRO for the model.

Note Added in Proof

The structure of the porcine FAS was solved at 4.5 Å resolution during the proof stage of this paper (Maier, T., Jenni, S., and Ban, N. Architecture of Mammalian Fatty Acid Synthase at 4.5 Å Resolution. *Science* 311:1258–1262). It reveals that the FAS is organized as a head-to-head homodimer and establishes that the overall quaternary structure of the β-carbon processing enzymes is as we propose here. It also shows that DH has a double hotdog fold and that KR shares an interface with it. Ban and co-workers were unable to fit the density adjacent to the catalytic subdomain of KR and suggest that it might be from ACP or TE. Our structural data show that it is from the structural subdomain of KR.